

NP-11-0036
August 4, 2011

10 CFR 52, Subpart A

U.S. Nuclear Regulatory Commission
ATTN: Document Control Desk
Washington, DC 20555-0001

Subject: Exelon Nuclear Texas Holdings, LLC
Victoria County Station Early Site Permit Application
Response to Request for Additional Information Letter No. 10
NRC Docket No. 52-042

Attached are responses to NRC staff questions included in Request for Additional Information (RAI) Letter No. 10, dated May 24, 2011, related to Early Site Permit Application (ESPA), Part 2, Sections 02.05.04, 02.05.05, 11.02 and 11.03. NRC RAI Letter No. 10 contained thirty-six (36) Questions. This submittal comprises the final partial response to RAI Letter No. 10, and includes responses to the following five (5) Questions:

02.05.04-13	02.05.05-2
02.05.04-14	02.05.05-3
	02.05.05-8

When a change to the ESPA is indicated by a Question response, the change will be incorporated into the next routine revision of the ESPA, planned for no later than March 31, 2012.

Of the remaining thirty-one (31) RAIs associated with RAI Letter No. 10, responses to eight (8) Questions were submitted to the NRC in Exelon Letter NP-11-0026, dated June 23, 2011, responses to twelve (12) Questions were submitted to the NRC in Exelon Letter NP-11-0029, dated July 8, 2011, and responses to eleven (11) Questions were submitted to the NRC in Exelon Letter NP-11-0034, dated July 25, 2011. This submittal completes the Exelon response to NRC RAI Letter No. 10, dated May 24, 2011.

Regulatory commitments established in this submittal are identified in Attachment 6.

If any additional information is needed, please contact David J. Distel at (610) 765-5517.

I declare under penalty of perjury that the foregoing is true and correct. Executed on the 4th day of August, 2011.

Respectfully,

A handwritten signature in black ink, appearing to read "Marilyn C. Kray". The signature is fluid and cursive, with the first name "Marilyn" written in a larger, more prominent script than the last name "Kray".

Marilyn C. Kray
Vice President, Nuclear Project Development

Attachments:

1. Question 02.05.04-13
2. Question 02.05.04-14
3. Question 02.05.05-2
4. Question 02.05.05-3
5. Question 02.05.05-8
6. Summary of Regulatory Commitments

cc: USNRC, Director, Office of New Reactors/NRLPO (w/Attachments)
USNRC, Project Manager, VCS, Division of New Reactor Licensing (w/Attachments)
USNRC Region IV, Regional Administrator (w/Attachments)

RAI 02.05.04-13:**Question:**

In accordance with 10 CFR 100.23(d)(4), the staff request that the applicant provide the following information regarding settlement:

- a) SSAR Table 2.5.4-89 presents the calculated and allowable settlements. This table states that settlement is 'N/A.' However, the calculated settlements at the center of the reactor/fuel building are on the order of 5 inches. Explain how settlement will be addressed, and the allowable bearing capacities that were assumed. Please discuss the underlying assumptions associated with estimating settlement and provide a sample calculation including the layer profile, elastic moduli, and the assumed depth used in the analysis.
- b) SSAR Subsection 2.5.4.10.3 states that the estimated settlement caused by the placement of the fill is approximately 0.8 inches and should occur relatively rapidly. This settlement was not included in the settlement calculations for Category I structures. Justify why this settlement was not taken into consideration knowing that it will affect the preconsolidation pressure for settlement calculations of the Category 1 structures. Also, describe how this settlement is included in the rebound/heave estimate for excavation of major power block area structures and how the 0.7 inch value was computed.

Response:**Part (a)**

SSAR Table 2.5.4-89 consists of two sets of settlement values. One set is the calculated settlement values, which will be addressed later in this response. The other set is the allowable settlement value specified by the technology vendor. The "Typical LWR with an Integral UHS" being cited here is based on the ESBWR, and Table 2.0-1 of Revision 6 of the ESBWR DCD provides the allowable settlement values contained in Table 2.5.4-89. DCD Table 2.0-1 does not provide any values for allowable settlement beneath the center of the structure. Thus, 'NA' was indicated in Table 2.5.4-89.

Note that, according to DCD Table 2.0-1, the allowable settlements (provided in Table 2.5.4-89) are post-construction settlements, except for the differential settlements within the structure, which are the allowable settlements after the basemat is poured. The calculated settlements in Table 2.5.4-89 are settlements that are anticipated during construction. Because of the elastic nature of the soils, little or no post-construction settlement is expected. For large heavy structures like the Reactor Building, there is a relatively constant relationship between corner, edge and center settlements. Thus, if the calculated edge settlement is well within the allowable limits (as shown in Table 2.5.4-89), the center settlement will also be within the allowable limits. As noted in SSAR Section 2.5.4.10.3, the settlement calculation assumes a flexible foundation. For the Reactor Building in particular, the foundation is relatively rigid. Thus, the 5 inches of settlement predicted at the center of the structure is an overestimate, and the actual settlement will be less.

The applied bearing pressures used to obtain the calculated settlements in Table 2.5.4-89 are the Maximum Static Bearing Demand values given in ESBWR DCD Table 2.0-1, namely 14.6 ksf for the Reactor/Fuel Building, 6.1 ksf for the Control Building, and 3.45 ksf for the Firewater Service Complex (rounded up to 3.5 ksf in the calculation).

A sample settlement calculation, provided below, shows how the settlement of the Unit 1 Reactor/Fuel Building was computed. The main features of this sample settlement calculation are described here. Table 1 and Figure 1 of the calculation show the subsurface profile below the Unit 1 Reactor/Fuel Building. Table 2 shows the estimated preconsolidation pressure in each clay layer and the total applied pressure at the center of each layer, which is the sum of the in-situ overburden pressure and the applied structure pressure from the Unit 1 Reactor/Fuel Building. The preconsolidation pressure exceeds the total applied pressure in each clay layer. This is the basis of using an elastic approach to computing settlement in these overconsolidated clay layers.

Equation 1 of the calculation is used for computing settlement in the layers beneath the foundation. Equation 2 is used to compute the stress from the foundation at selected depths beneath the corner of the foundation using a Boussinesq-type distribution. Stress is computed beneath other points in the foundation by superposition. The σ_z computed in Equation 2 is used as input p_i in Equation 1. Typically, the computation extends to a depth where the increase in vertical stress due to the applied load is equal to or less than 10% of the applied load.

Table 3 of the calculation lists selected engineering properties of the soils in each layer. These include the estimated high-strain and low-strain shear modulus (G) and elastic modulus (E) for each layer. The low-strain modulus is typically at a strain of $10^{-4}\%$. The high-strain modulus is typically in the 0.25% to 0.5% strain range, but can be taken as high as 1%. The right-hand column of Table 3 is labeled " G/G_{\max} Reduction Curve" and assigns a curve to each soil layer. G_{\max} is the low-strain shear modulus. The G/G_{\max} versus shear strain curves are shown in Figure 2 of the calculation. Note that Figure 2 labels the vertical axis " G/G_{\max} and E/E_{\max} " and the horizontal axis "Shear Strain, γ & Vertical Strain, ϵ_v , %". Thus, these curves also represent the variation of elastic modulus with vertical strain. This variation is taken into account in the settlement calculation. For the first iteration of the calculation, the low-strain elastic modulus value (E_{\max}) is assumed for each layer and the settlement in each layer is computed, using an Excel spreadsheet. This settlement is divided by the layer thickness to determine the vertical strain, ϵ_v , in the layer. The elastic modulus corresponding to this strain is then found from the appropriate E/E_{\max} versus ϵ_v curve for the layer, and a second iteration of the settlement computation is made. The process is repeated until the change in computed settlement between iterations becomes negligible. The various E/E_{\max} versus ϵ_v curves are digitized and stored in the Excel spreadsheet, and the iterative process is programmed into the spreadsheet. The same iterated settlement would have been obtained starting with the high-strain elastic modulus since the procedure iterates to the elastic modulus that has the same vertical strain from the elastic modulus curves as the vertical strain calculated from the settlement of the soil layer. Since the elastic modulus reduction curves have a maximum vertical strain of 1 percent the initial elastic modulus chosen to start the procedure must have a corresponding strain of < 1 percent to perform the calculation. Note that the high-strain modulus was conservatively assumed for the fill at all strain levels.

Sample Settlement Calculation

SSAR Table 2.5.4-89 provides values of calculated settlement for various structures. For the Unit 1 Reactor/Fuel building, for the "Clay Preferred" soil profile, the calculated settlements are 2.7 in., 1.5 in. and 5.0 in. under the edge, corner and center of the foundation, respectively. This sample calculation demonstrates how these settlement values were computed. The sample calculation includes the soil layer profile, the assumed depth and the elastic moduli that were used.

Soil Layer Profile

When considering the soil layer profile, since more than one type of subsurface material can be located in the same elevation range due to uneven topography, two soil profiles are generated, with the soil selection processes being labeled "Clay Preferred" or "Sand Preferred". With the soil selection label of "Clay Preferred", the clay stratum below the respective foundation and its characteristic elastic modulus represent the elevation range containing the two soil types. Similarly, for soil profiles with the label "Sand Preferred", the sand stratum below the respective foundation and its characteristic elastic modulus represents the elevation range containing the two soil types. In this sample calculation for the Unit 1 Reactor building, there is minimal difference between the "Clay Preferred" and "Sand Preferred" profiles, and the computed settlements, as shown in Table 2.5.4-89, are the same after rounding.

Table 1: Information on the approximate subsurface profile below the Unit 1 Reactor/Fuel building foundation

Simplified Soil Profile						Soil Profile for Calculation	
Depth (ft)		Elevation (ft)		Thickness (ft)	Soil Layer	Clay Preferred	Sand Preferred
Top	Bottom	Top	Bottom				
65.6	87.0	29.4	8.0	21.4	Fill	Fill	Fill
87.0	103.0	8.0	-8.0	16.0	Clay 3	Clay 3	Clay 3
103.0	118.0	-8.0	-23.0	15.0	Sand 4	Sand 4	Sand 4
118.0	150.0	-23.0	-55.0	32.0	Clay 5	Clay 5	Clay 5
150.0	175.0	-55.0	-80.0	25.0	Clay 5/Sand 6	Clay 5	Sand 6
175.0	220.0	-80.0	-125.0	45.0	Sand 6	Sand 6	Sand 6
220.0	255.0	-125.0	-160.0	35.0	Clay 7	Clay 7	Clay 7
255.0	300.0	-160.0	-205.0	45.0	Sand 8	Sand 8	Sand 8
300.0	337.0	-205.0	-242.0	37.0	Clay 9	Clay 9	Clay 9
337.0	350.0	-242.0	-255.0	13.0	Sand 10	Sand 10	Sand 10
350.0	422.0	-255.0	-327.0	72.0	Clay 11	Clay 11	Clay 11
422.0	440.0	-327.0	-345.0	18.0	Sand 12	Sand 12	Sand 12
440.0	516.0	-345.0	-421.0	76.0	Clay 13	Clay 13	Clay 13
516.0	549.0	-421.0	-454.0	33.0	Sand 14	Sand 14	Sand 14
549.0	560.0	-454.0	-465.0	11.0	Clay 15	Clay 15	Clay 15
560.0	575.0	-465.0	-480.0	15.0	Sand 16	Sand 16	Sand 16
575.0	600.0	-480.0	-505.0	25.0	Clay 17	Clay 17	Clay 17

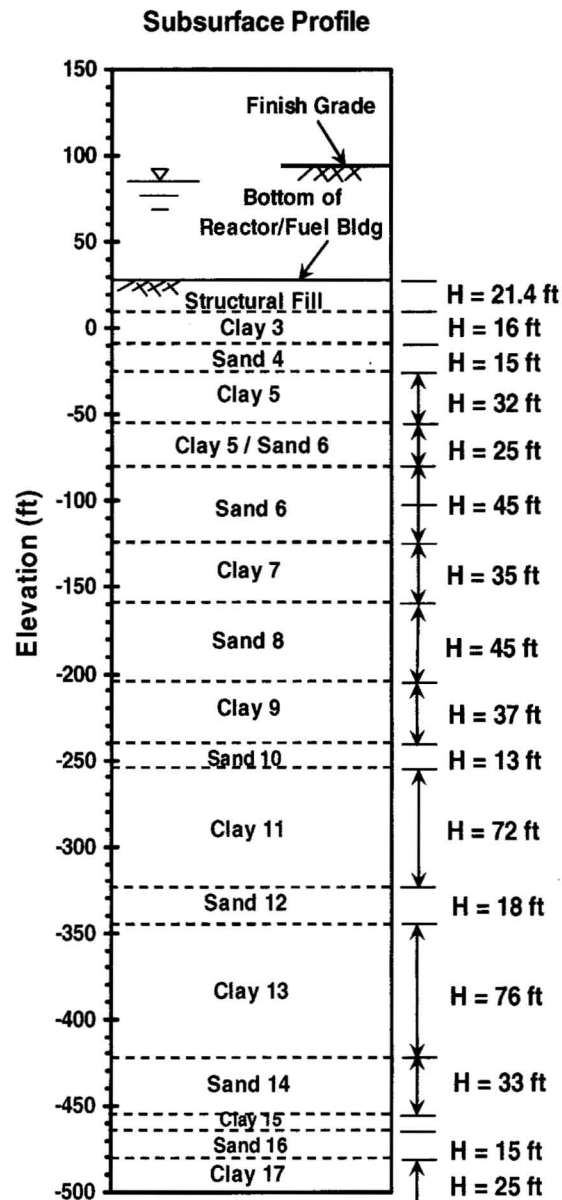


Figure 1: Subsurface profile beneath the Unit 1 Reactor/Fuel building

The subsurface profile tabulated in Table 1 is shown in Figure 1.

Computation Method Selected

The settlement produced by loading on the soil can best be estimated by assuming either pseudo-elastic compression or one-dimensional consolidation. For granular soils or overconsolidated cohesive soils, the settlement can be calculated assuming pseudo-elastic compression.

Assuming that the distribution of stress increase resulting from the load follows a 2:1 (V:H) slope (Perloff, 1975), Table 2 shows the vertical stress from the application of the design

load and the preconsolidation stress of the soils beneath the Unit 1 Reactor/Fuel building. For the soil layer that consists of both clayey and sandy material, the clayey soil is selected to represent the layer for the Clay Preferred calculations. Comparison shows that the preconsolidation stress of each soil layer is higher than the total vertical effective stress at the mid-depth of the layer. This is true even if the 2.1 ksf due to the planned 15 ft of fill to raise site grade is added. Therefore, there is no virgin compression in the soils upon loading, and the total settlement results from only recompression, which can be estimated using the elastic method. Note that the groundwater table was assumed to be at El. 48 ft in Table 2, giving a higher, and thus more conservative, estimate of effective stress than at El. 85 ft, the predicted maximum groundwater level after the cooling reservoir is constructed and filled.

Table 2: Comparison of the preconsolidation stress with the vertical stress below the Unit 1 Reactor/Fuel building

Simplified Soil Profile				Selected Soil Profile (Clay Preferred)			Vertical Stress at Mid-Depth of Soil Layers						
Elevation (ft)		Thickness (ft)	Soil Layer	Soil Layer	Unit Weight, γ (pcf)	Preconsolidation Pressure, σ _p ' (ksf)	Width, B' (ft)	Length, L' (ft)	Loading, σ (ksf)	Overburden, σ _{vo} (ksf)	Pore Pressure, u (ksf)	Total Effective Stress, σ' _v (ksf)	
Top	Bottom												
29.4	8	21.4	Fill	Fill	138	-	172	241	13.1	1.5	1.8	12.7	
8	-8	16	Clay 3	Clay 3	119	16	190	259	10.9	3.9	3.0	11.9	
-8	-23	15	Sand 4	Sand 4	132	-	206	275	9.6	5.8	4.0	11.4	
-23	-55	32	Clay 5	Clay 5	127	20	229	298	7.9	8.9	5.4	11.3	
-55	-80	25	Clay 5/Sand 6	Clay 5	127	20	258	327	6.4	12.5	7.2	11.7	
-80	-125	45	Sand 6	Sand 6	132	-	293	362	5.1	17.0	9.4	12.8	
-125	-160	35	Clay 7	Clay 7	125	25	333	402	4.0	22.2	11.9	14.4	
-160	-205	45	Sand 8	Sand 8	132	-	373	442	3.3	27.4	14.4	16.3	
-205	-242	37	Clay 9	Clay 9	126	35	414	483	2.7	32.7	16.9	18.4	
-242	-255	13	Sand 10	Sand 10	132	-	439	508	2.4	35.9	18.5	19.8	
-255	-327	72	Clay 11	Clay 11	119	40	481	550	2.0	41.0	21.2	21.9	
-327	-345	18	Sand 12	Sand 12	132	-	526	595	1.7	46.5	24.0	24.2	
-345	-421	76	Clay 13	Clay 13	126	45	573	642	1.5	52.4	26.9	27.0	
-421	-454	33	Sand 14	Sand 14	132	-	628	697	1.2	59.4	30.3	30.3	
-454	-465	11	Clay 15	Clay 15	126	47	650	719	1.2	62.3	31.7	31.8	
-465	-480	15	Sand 16	Sand 16	132	-	663	732	1.1	64.0	32.5	32.6	
-480	-505	25	Clay 17	Clay 17	131	50	683	752	1.1	66.6	33.7	33.9	

Settlement Calculation Using Elastic Method

Based on a stress-strain model that computes settlement in discrete layers, the settlement, δ , of shallow foundations due to elastic compression of the subsurface materials can be calculated as follows:

$$\delta = \sum(p_i \times h_i)/E_i \quad (\text{Equation 1})$$

where: δ = settlement

$i = 1$ to n , where n is the number of layers

p_i = vertical applied pressure at center of layer i

h_i = thickness of layer i

E_i = elastic modulus of layer i

The stress distribution below a rectangular foundation is based on a Boussinesq-type distribution provided in Poulos & Davis (1974) for flexible foundations. The Boussinesq-type vertical pressure under the corner of a rectangular footing, σ_z , is as follows:

$$\sigma_z = (p/2\pi)\{\tan^{-1}[lb/(zR_3)] + (lbz/R_3)(1/R_1^2 + 1/R_2^2)\} \quad (\text{Equation 2})$$

where: p = applied foundation pressure

l = length of the footing

b = width of footing

z = depth below footing at which pressure is computed

$$R_1 = (l^2 + z^2)^{0.5}$$

$$R_2 = (b^2 + z^2)^{0.5}$$

$$R_3 = (l^2 + b^2 + z^2)^{0.5}$$

The pressure under the center or edge of the foundation is obtained by superposition. For example, to compute the vertical pressure beneath the center of a rectangular foundation, the rectangle is divided into 4 equal rectangles each with a corner at the center. The vertical pressure under the corner of one rectangle is computed, and multiplied by 4 to obtain the total pressure under the center.

An Excel spreadsheet has been developed to automate the computation process for settlement. The computation extends to a depth where the increase in vertical stress under the center of the foundation due to the applied load is equal to or less than 10% of the applied load.

Strain-Dependent Elastic Modulus

Typically, settlement calculations use the high-strain elastic modulus (E_s). For large structures such as the Reactor/Fuel building where the significant zone of influence of the load extends several hundred feet below the foundation, the vertical strain in the soil in the deeper layers is small, and the use of E_s can be overly conservative. Swiger (1974) states that a modulus reduction of 1/3 is appropriate for heavy structures where anticipated strain is on the order of 10^{-3} inches/inch. In the strain-dependent elastic modulus approach, the value of elastic modulus corresponding to the vertical strain in the layer is used.

For the settlement calculation of structures using the elastic method, the maximum principal strain is the vertical strain (i.e., $\epsilon_1 = \epsilon_v$), while the minimum principal strain is assumed to be zero (i.e., $\epsilon_3 = 0$). Since the maximum shear strain $\gamma_{\max} = \epsilon_1 - \epsilon_3 = \epsilon_1$ (Poulos & Davis, 1974) and $E/E_{\max} = G/G_{\max}$, where E_{\max} and G_{\max} are the low-strain elastic and shear modulus values, respectively, the elastic modulus reduction curves with respect to vertical strain should be the same as the shear modulus reduction curves with respect to the shear strain. Based on results of resonant column - torsional shear tests (RCTS) on the soil samples, the shear modulus reduction curves indicated in Table 3 are recommended. These are plotted in Figure 2. Table 3 also contains the values of high- and low-strain shear and elastic modulus of each layer.

With an assumed initial elastic modulus E_0 an initial settlement calculation is done and the corresponding vertical strain ϵ_{v0} is calculated as $\epsilon_{v0} = \delta_0/h$, where h is the thickness of the soil layer and δ_0 is the settlement of the soil layer. Based on ϵ_{v0} , the elastic modulus E_1 is derived from the elastic modulus reduction curves. E_1 is then used in the settlement calculation and the iteration process continues until compatible elastic modulus and vertical strain are found.

Table 3: Selected engineering properties of the subsurface materials

Soil Stratum	Undrained Shear Strength, s_u (ksf)	Friction Angle, ϕ' (°)	Preconsolidation Pressure, σ_p' (ksf)	Unit Weight, γ (pcf)	Poisson's Ratio, ν	Shear Modulus		Elastic Modulus		G/G _{max} Reduction Curve
						High Strain, G_s (ksf)	Low Strain, G_{max} (ksf)	High Strain, E_s (ksf)	Elastic Modulus, E_{max} (ksf)	
Clay 1	3.2	-	10	129	0.45	690	2502	2000	7256	PI = 70
Sand 1	-	33	-	135	0.44	446	4872	1160	14031	Depth < 50 ft
Sand 2	-	33	-	135	0.475	415	4731	1080	13956	Depth > 50 ft
Clay 3	3	-	16	119	0.485	807	3623	2340	10760	PI = 200
Sand 4	-	37	-	132	0.46	900	10416	2340	30415	Depth > 50 ft
Clay 5	3	-	20	127	0.48	1072	5143	3110	15223	PI = 200
Sand 5	-	36	-	132	0.475	654	7656	1700	22585	Depth > 50 ft
Sand 6	-	39	-	132	0.47	869	8936	2260	26272	Depth > 50 ft
Clay 7	6	-	25	125	0.47	1679	7935	4870	23329	PI = 200
Sand 8	-	36	-	132	0.465	1088	11263	2830	33001	Depth > 50 ft
Clay 9	4	-	35	126	0.48	1297	6132	3760	18151	PI = 200
Sand 10	-	38	-	132	0.46	1292	11042	3360	32243	Depth > 50 ft
Clay 11	5	-	40	119	0.48	1234	4865	3580	14400	PI = 200
Sand 12	-	36	-	132	0.455	1096	13478	2850	39221	Depth > 50 ft
Clay 13	6	-	45	126	0.47	1721	7328	4990	21544	PI = 200
Sand 14	-	36	-	132	0.45	1150	13860	2990	40194	Depth > 50 ft
Clay 15	6.1	-	47	126	0.47	2024	8820	5870	25931	PI = 200
Sand 16	-	38	-	132	0.455	1123	12901	2920	37542	Depth > 50 ft
Clay 17	5.6	-	50	131	0.46	2307	13084	6690	38205	PI = 70
Sand 18	-	38	-	132	0.45	1508	16316	3920	47316	Depth > 50 ft
Fill	-	39	-	138	0.35	400	3320	1100	8964	-

Note: For the G/G_{max} reduction curves, "PI = 70" indicates the PI = 70 curve suggested by EPRI (1993), "PI = 200" indicates the PI = 200 curves suggested by Vucetic & Dobry (1991), and "Depth > 50 ft" and "Depth < 50 ft" indicate the corresponding curves suggested by Silva et al. (1997).

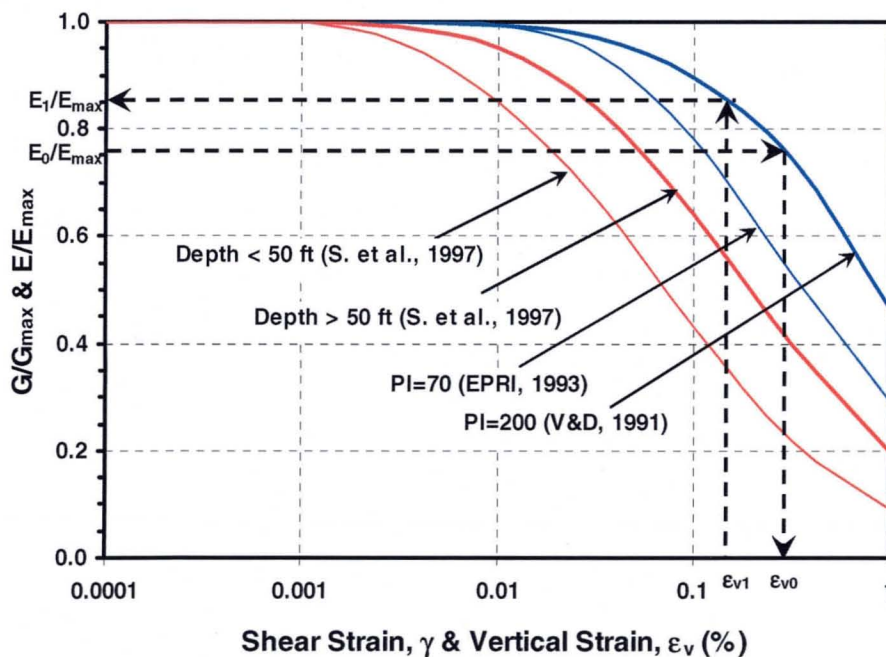


Figure 2: Elastic modulus reduction curves

Calculation of Settlement of Unit 1 Reactor/Fuel Building

The spreadsheet used to compute the settlement using the strain-dependent method is shown in Table 4. This uses the "Clay Preferred" soil layer profile, but, as noted earlier, the settlement values obtained using the "Sand Preferred" profile is almost identical. The fourth column of the spreadsheet shows the low-strain elastic modulus (E_{\max}) used in the first iteration of settlement. The exception is the structural fill where, although the E_{\max} value is included, the high-strain value of E (1,100 ksf) was used for each iteration. The computed strain for the final iteration is shown in the "Strain (%)" column. The next column shows the corresponding E/E_{\max} from Figure 2. The curve from Figure 2 was digitized and put into the spreadsheet to perform the iteration process. The next column shows the E value used in the final iteration. For example, for Sand 4, $E_{\max} = 30,415$ ksf. For the calculation of center settlement, the strain at the final iteration is 0.061 percent. The corresponding E/E_{\max} shown is 0.73 (rounded from 0.7339 actually computed), and the final E value is $0.7339 \times 30,415 = 22,322$ ksf.

References

EPRI (1993). "Guidelines for Determining Design Basis Ground Motions", Vols. 1-5, EPRI TR-102293, Electric Power Research Institute, Palo Alto, CA.

Perloff, W.H. (1975). "Pressure Distribution and Settlement", in *Foundation Engineering Handbook*, H.F. Winterkorn and H-Y Fang, Editors, Van Nostrand Reinhold Co., New York.

Poulos, H.G., and Davis, E.H. (1974). *Elastic Solutions for Soil and Rock Mechanics*, John Wiley, New York.

Silva, W. J., Abrahamson, N.A, Toro, G.R. and Constantino, C.J. (1997). "Description and Validation of the Stochastic Ground Motion Model", Contract 770573, Report to Brookhaven National Laboratory, Associated Universities, Inc., Upton, New York.

Swiger W.F., (1974). "Evaluation of Soil Moduli," Proceedings, Analysis and design in Geotechnical Engineering, Vol. 2, University of Texas-Austin, pp. 79-92.

Vucetic, M. and R. Dobry (1991). "Effect of Soil Plasticity on Cyclic Response," Journal of Geotechnical Engineering, ASCE, Vol. 117, No. 1, January.

Table 4: Settlement computation for the Unit 1 Reactor/Fuel building using the strain-dependent elastic modulus

[illegible]

Part (b)

As described in the response to (a), an elastic approach to calculating the settlement of the overconsolidated clays was adopted because the preconsolidation pressure in these soils was greater than the in-situ pressure due to overburden pressure and applied foundation pressure. There will be no significant change in the elastic modulus values of the overconsolidated clays and sands used in the settlement computation, either due to the addition of 15 ft of fill at the surface, or due to the excavation of soils for the deeper structures. Consequently, there will be no significant change in calculated settlement.

Based on engineering judgment, the assumption is reasonable that the 0.8 inches of settlement predicted from placing the 15 ft of fill will occur relatively rapidly, as it will be elastic settlement, and will be complete before construction of the major structures starts. Thus, the actual settlement experienced by the structures will be independent of the 0.8 inches. When settlement monitoring begins for these structures during construction, it will not take account of the 0.8 inches of settlement due to the fill.

The amount of heave is a function of the depth of excavation required to construct the foundation. (This is unlike the amount of settlement that will occur due to raising the site grade 15 ft, which is independent of the technology adopted and the depths of the structures involved.) The 0.7 inches value of predicted heave is based on the estimated removal of 7.1 ksf of overburden soil. Because the elastic modulus of the overconsolidated soils is assumed to be the same whether pressure is applied or relieved, the same approach is used for computing heave as for computing settlement.

Excavation of the major power block structures will be over a reasonably long period of time, and accordingly it is assumed that all of the predicted foundation heave will have occurred before foundation construction starts. Thus, the 0.7 inches of predicted heave is not included in the predicted foundation settlement. Settlement due to the placement of 15 ft of fill is assumed to have occurred before excavation, and hence heave, starts. Although this assumption depends on construction sequence and it is possible that the 15 ft of fill will not be placed over the power block structure area and that excavation of the power block will occur during fill placement, the calculated structure settlements are not anticipated to be affected. This is because the soils on site are made up of overconsolidated clays and dense sands and the settlement and heave due to the fill and excavation will both occur before foundation construction begins regardless of the order in which they are completed.

Although the pressure used to compute heave beneath the Reactor Building is almost half of the pressure used to compute the Reactor Building settlement, the computed heave beneath the center of the structure is only 0.7 inches, compared with 5 inches computed settlement. The reason for this large difference is that the settlement calculation includes the settlement of approximately 22 ft of fill, placed immediately below the structure. The computed settlement of this fill is approximately 3.5 inches. The remaining 1.5 inches of settlement of the underlying soil due to the 14.6 ksf applied loading is in good agreement with the 0.7 inches of heave due to 7.1 ksf of excavation.

Note that the last paragraph of SSAR Section 2.5.4.10.3 indicates that the maximum excavation for the deepest structure considered is 110 ft, and that the maximum rebound/heave for excavation of major power block area structures is estimated at 0.7 inches. In fact, as discussed above, the 0.7 inches heave was computed for the Typical

LWR with an Integral UHS, with a maximum excavation of about 72 ft below existing grade and 87 ft below final grade. The SSAR section will be modified to clarify this.

Associated ESPA Revisions:

The last paragraph of SSAR Section 2.5.4.10.3 will be updated in a future revision to the ESPA as indicated:

Also note that unloading of the soil profile results from mass excavation for power block area major structures (i.e., maximum 72 feet below existing grade, 87 feet below final grade for the structures with calculated settlements presented in Table 2.5.4-89 ~~110 feet of excavation for the deepest structure considered~~). This unloading results in rebound/heave of the base of the excavation, which is monitored/accounted for during construction. ~~Maximum~~ Rebound/heave for excavation of major power block area structures included in Table 2.5.4-89 is estimated ~~at~~ to be less than or equal to 0.7 inches.

RAI 02.05.04-14:**Question:**

In accordance with 10 CFR 100.23(d)(4), the staff request that the applicant provide the following information regarding lateral earth pressure evaluations:

- a) SSAR Subsection 2.5.4.10.4 states that “vertical ground accelerations are considered negligible.” Please explain this statement.
- b) SSAR Subsection 2.5.4.10.4.2 states that: “Since the VCS site employs highly compacted granular structural fill with relatively low permeability, seismic groundwater pressure need not be considered. Therefore, only the static water level is considered in calculating the hydrostatic groundwater pressure, as given in Equation 2.5.4-36. Note that seismic groundwater thrust greater than 35 percent of hydrostatic thrust can develop for cases when $kh > 0.30g$ (Reference 2.5.4-66). Given the relatively low seismicity of the VCS site (i.e., $kh < 0.30g$), seismic considerations related to groundwater can similarly be disregarded.” Please justify this assumption the seismic considerations can be disregarded for all designs considered in the PPE and provide sample calculations, including the hydrodynamic thrust.

Response:**Part (a)**

The statement “vertical ground accelerations are considered negligible” in SSAR Subsection 2.5.4.10 is in the context of seismic active earth pressures. Figure 15 of Seed and Whitman (1970) shows the effect of vertical ground acceleration ($k_v g$) on the dynamic earth pressure coefficient, where g is acceleration due to gravity. This assumes (1) a vertical wall with level backfill behind the wall; (2) an angle of internal friction for the backfill of 35 degrees; and (3) an angle of wall friction of 2/3 of the angle of internal friction. For horizontal ground acceleration of 0.1g with no vertical acceleration, the dynamic earth pressure coefficient (K_{AE}) is 0.3. For a downwards vertical ground acceleration of 0.1g ($k_v = +0.1$), K_{AE} is about 0.32, and for an upwards vertical ground acceleration of 0.1g ($k_v = -0.1$), K_{AE} is about 0.28.

Equation 1 of Seed and Whitman (1970) shows the total active earth pressure, P_{AE} during an earthquake is:

$$P_{AE} = 0.5\gamma H^2(1-k_v)K_{AE}$$

Where γ = total unit weight of backfill
 H = height of the wall
 k_v = (vertical ground acceleration)/g

Based on this equation:

when $k_v = +0.1g$ (downwards), then $(1-k_v)K_{AE} = 0.9 \times 0.32 = 0.29$
 when $k_v = -0.1g$ (upwards), then $(1-k_v)K_{AE} = 1.1 \times 0.28 = 0.31$

This demonstrates that the effect of vertical acceleration in this situation is small and can be neglected.

Part (b)

The response to RAI 02.05.04-5 provides details of the type of structural backfill that will be used on the project. The sandy gravels in Samples 1 and 2 have high maximum dry unit weight values (133 and 136.5 pcf) with optimum moisture content around 6 percent. These are very well graded materials with high values of coefficient of uniformity. This means that the soil particles are very tightly packed and the material, although granular, will have relatively low permeability. During an earthquake, the pore water within the soil (around 20 percent by volume when below the water table) will not behave independently of the soil skeleton – the soil and water will act as one unit.

With a uniform well-drained coarse sand or gravel, where the pore water is free to move independently of the soil skeleton, the dynamic component of lateral pressure will be made up of the dynamic earth pressure based on the effective weight of the soil, plus the hydrodynamic thrust from the pore water. For the well-graded VCS compacted structural fill where the pore water and soil skeleton act together (i.e., undrained behavior), the dynamic component of lateral pressure will be made up of the dynamic earth pressure based on the total weight of the soil. There will be no hydrodynamic thrust from the pore water. This difference between well-drained and undrained behavior with respect to dynamic water pressure is summarized in Whitman (1990). Thus, no calculations for the hydrodynamic thrust were completed.

Response Reference:

Seed, H.B., and R.V. Whitman (1970). "Design of Earth Retaining Structures for Dynamic Loads," *Proceedings of the Specialty Conference on Lateral Stresses in the Ground and Design of Earth Retaining Structures*, American Society of Civil Engineers, New York. (SSAR Reference 2.5-63)

Whitman, R.V. (1990). "Seismic Design and Behavior of Gravity Retaining Walls," *Proceedings of the Specialty Conference on Design and Performance of Earth Retaining Structures*, American Society of Civil Engineers, New York. (SSAR Reference 2.5-66)

Associated ESPA Revisions:

The following correction will be made in SSAR Section 2.5.4.13 (References) in a future revision of the ESPA:

2.5.4-66 Whitman, R.V. Seismic Design and Behavior of Gravity Retaining Walls, *Proceedings of the Specialty Conference on Design and Performance of Earth-Retaining Structures*, American Society of Civil Engineers, NY, 1990.

RAI 02.05.05-2:**Question:**

SSAR Subsection 2.5.5.1.9.1.1 states that the values of undrained shear strength obtained from the direct simple shear tests showed greater consistency than those obtained from the isotropically-consolidated undrained (CIU) saturated triaxial compression test. In accordance with 10 CFR 100.23(d)(4), please explain the possible reasons on why the CIU results were inconsistent.

Response:

SSAR Subsection 2.5.5.1.9.1.1 discusses the results of CIU triaxial compression and direct simple shear (DSS) tests made on samples of the embankment fill, i.e., composite A and composite B. As explained in SSAR Subsection 2.5.4.5.1.1.2, for the cooling basin, test pit bulk samples representative of the sand soils and clay soils excavated and reused for embankment fill are selected and combined for laboratory testing of recompacted specimens, as follows:

- Composite "A"/Sand: a blend of bulk samples having similar properties obtained from two test pits (test pit TP-2319, bulk sample 2 and test pit TP-2334, bulk sample 2), and representative of the coarser-grained soils used for embankment fill. The combined/tested bulk sample is a clayey sand (USCS classification, SC) with fines content of 46 percent.
- Composite "B"/Clay: a blend of bulk samples having similar properties obtained from two test pits (test pit TP-2317, bulk sample 1 and test pit TP-2334, bulk sample 1), and representative of the finer-grained soils used for embankment fill. The combined/tested bulk sample is a lean clay with sand (USCS classification, CL) with fines content of 74 percent.

Interpretation of the CIU shear strength data is based on the total stress (p-q) parameters, which are defined in SSAR Figure 2.5.5-9. Three specimens from each composite material were tested at three different confining pressures. Figure 1 is a graphic presentation of the p-q data. Considering the relatively similar properties (clayey sand versus lean clay with sand) and compaction characteristics of the two composites, Figure 1 shows a considerable difference between the undrained shear strengths of the two composites, i.e., 1.4 ksf for composite A versus 0.7 ksf for composite B for p=0 ksf.

Figure 2 shows the variation of the DSS undrained shear strength with vertical effective stress. There is high degree of similarity between the results of the two composites. The best-fit trend line is represented in Figure 2. This behavior is in contrast with the CIU test data presented in Figure 1.

As discussed in SSAR Subsection 2.5.5.1.9.1, Reference 1 (SSAR Reference 2.5.5-4) shows that estimates of undrained shear strengths measured in triaxial compression tests are almost always unconservative because isotropic consolidation in the tests leads to a water content that is too low (which increases the measured strength), and because shearing in triaxial compression ignores anisotropy and therefore over-estimates strength.

The undrained shear strength results obtained from the DSS tests show consistency between the results as discussed above, whereas the triaxial test results indicate greater differences that suggest the DSS test results should be used to determine the undrained shear strength parameters for the embankment material.

Response Reference:

1. Ladd, C.C. and DeGroot, D.J., "Recommended Practice for Soft Ground Site Characterization: Arthur Casagrande Lecture," 12th Pan-American Conference on Soil Mechanics and Geotechnical Engineering, (Nonproprietary), Massachusetts Institute of Technology, Cambridge, Massachusetts, 2003.

Associated ESPA Revision:

No ESPA revision is required as a result of this response.

Figure 1: Diagram of p-q for composites A and B from isotropically consolidated undrained (CIU) triaxial tests

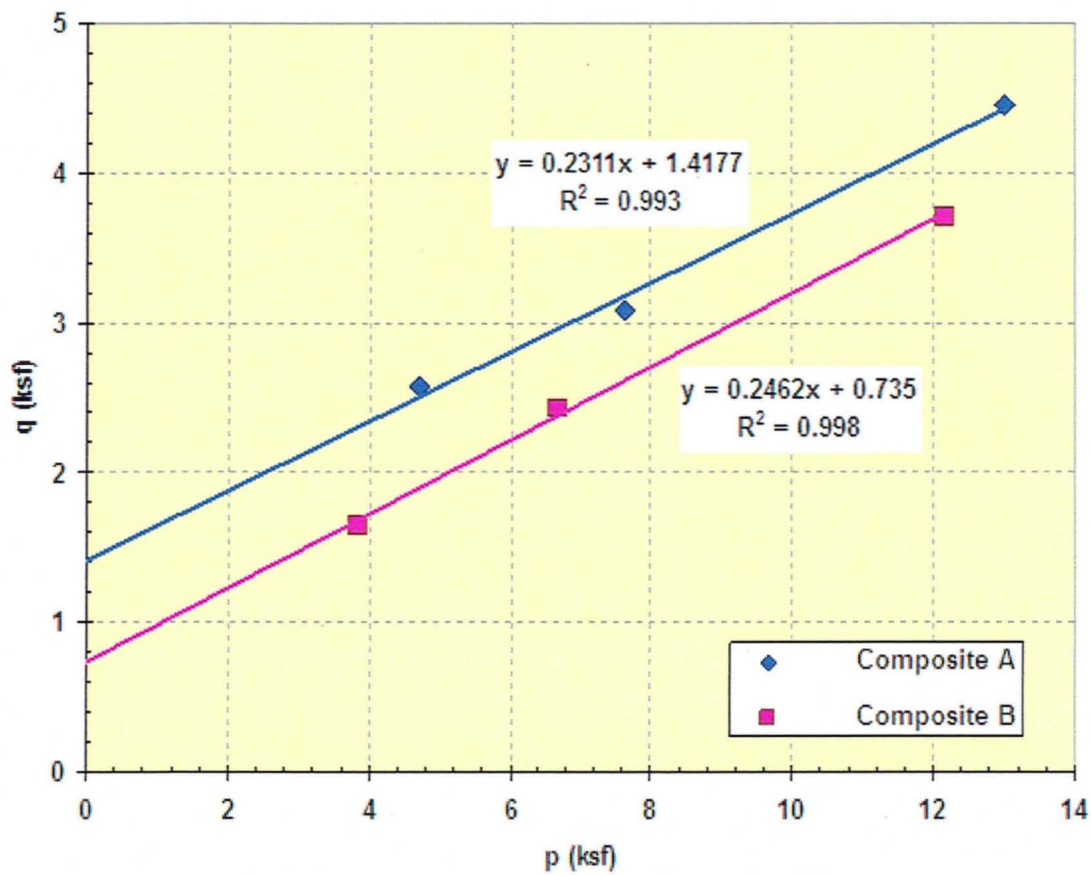
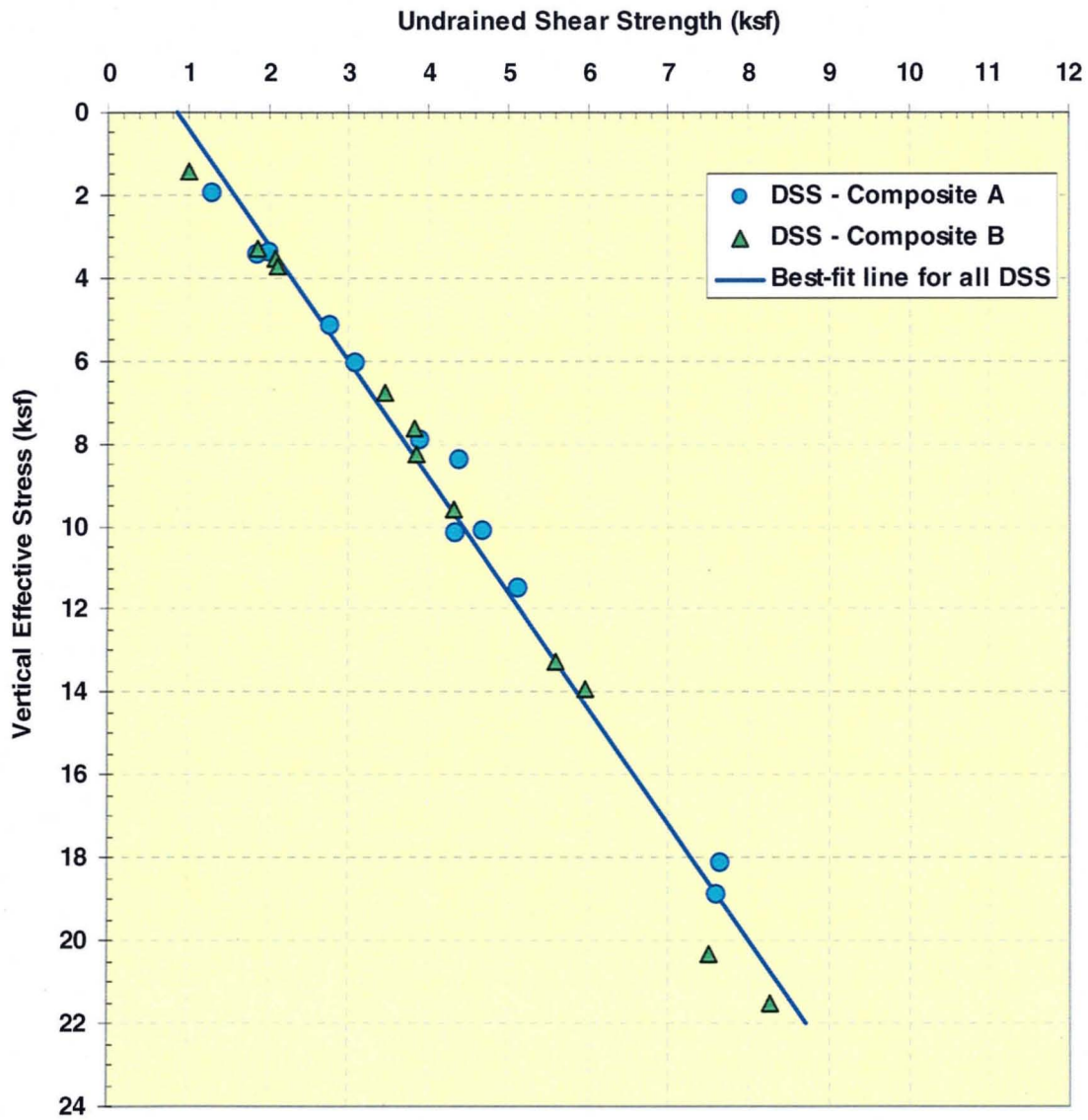


Figure 2: Undrained shear strength versus effective vertical stress for composites A and B from direct simple shear (DSS) tests



RAI 02.05.05-3:**Question:**

SSAR Subsection 2.5.5.1.11 indicates that shallow investigations disclosed the presence of a surficial loose layer of sand to the east of the cooling basin along the side of Linn Lake. The applicant concluded that this sand is beyond the limits of the embankment dam. In accordance with 10 CFR 100.23(d)(4), please explain how far beyond the limit this loose layer is located. Also, explain if this loose layer was considered in the slope stability analysis along the east embankment of the cooling basin.

Response:

Layers identified as loose sand were characterized in the liquefaction analysis discussed in SSAR Subsection 2.5.4.8. An assessment of the cooling basin soils against liquefaction was performed based on the SPT, CPT and shear wave velocity data, and the results were summarized in SSAR Subsections 2.5.4.8.2.2, 2.5.4.8.3.2, and 2.5.4.8.4.2, respectively. The test points where liquefaction potential was observed were tabulated in SSAR Tables 2.5.4-77, -79 and -81, along with the corresponding soil layers. SSAR Subsection 2.5.5.1.11 refers to these findings and indicates shallow investigations (~ 10 feet) disclosed the presence of surficial loose sand layers to the east of the cooling basin along the side of Linn Lake.

Note that for completeness purposes, all data points including both sand and clay layers were tabulated in SSAR Tables 2.5.4-77, -79 and -81. For this RAI response, SSAR Tables 2.5.4-77, -79 and -81 are re-iterated but modified in Table 1 so that only the sand layers on the order of 10 feet deep, located to the east of the cooling basin are presented. Table 1 also shows the depth of the test points where liquefaction potential was observed. From Table 1, test locations B-03, B-2324, B-2336, C-2307, C-2308, C-2319, C-2303S, and C-2323S are where loose surficial sand layers are identified. Figure 1 illustrates the locations of these boring/CPT and the corresponding distances with respect to the eastern embankment.

Any presence of loose sand layers was not included in the slope stability analysis, assuming that ground treatment will take place if needed. As indicated in Subsection 2.5.4.12, ground treatment along the alignment of the embankments is limited to localized over-excavation of unsuitable soils, such as minor zones of less competent soils occurring at embankment foundation subgrades, and their replacement with compacted embankment fill.

Associated ESPA Revisions:

No ESPA revision is required as a result of this response.

Table 1- Liquefaction evaluation of sand layers to the east of the cooling basin

Boring (Number of Test Points)	Test El. NAVD 88 (feet)	Test Depth (feet)	Factor of Safety (FOS)	Structure	Stratum (Disposition)
B-03 (1)	74.9	0.0	1.08	No Structure (East of CB)	Stratum Sand 1 (No structure)
B-2324 (1)	24.5	0.0	0.81	No Structure (East of CB)	Stratum Sand 2 (No structure)
B-2336 (1)	57.0	11.0	0.97	No Structure (East of CB)	Stratum Sand 1 (No structure)

Source: SSAR Table 2.5.4-77

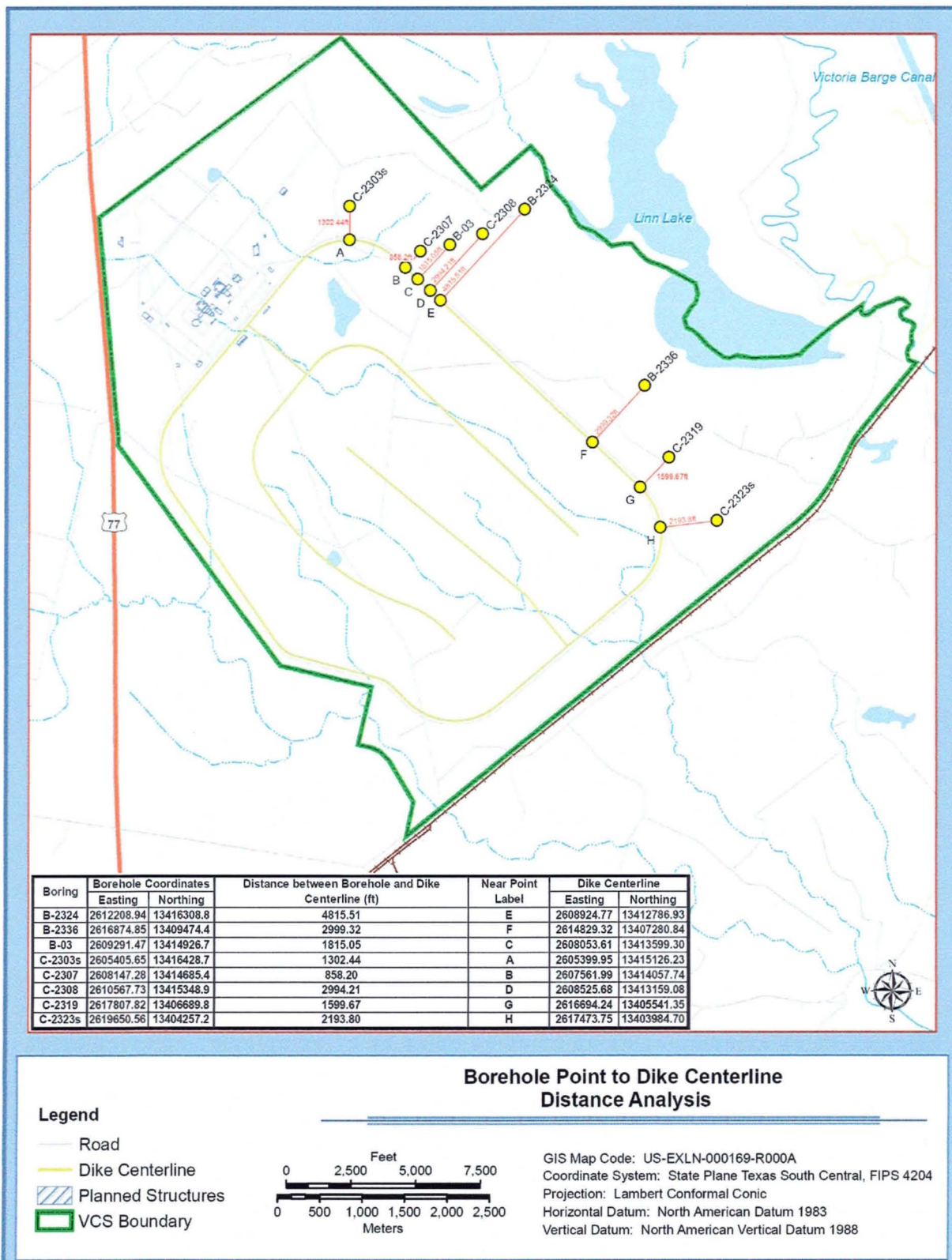
CPT (Number of Test Points)	Test El. NAVD 88 (feet)	Test Depth (feet)	Factor of Safety (FOS)	Structure	Stratum (Disposition)
C-2307 (5)	74.88 to 72.63	0 to 2.25	0.48 to 0.91	No Structure (East of CB)	Stratum Sand 1 (no structure)
C-2307 (1)	63.63	11.25	1.01	No Structure (East of CB)	Stratum Sand 1 (no structure)
C-2308 (9)	58.02 to 52.77	0 to 5.25	0.53 to 1.09	No Structure (East of CB)	Stratum Sand 1 (no structure)
C-2319 (2)	56.31 to 55.81	9.25 to 9.75	0.85 to 0.97	No Structure (East of CB)	Stratum Sand 1 (no structure)

Source: SSAR Table 2.5.4-79

V_s Boring/CPT (Number of Test Points)	Test El. NAVD 88 (feet)	Test Depth (feet)	Factor of Safety (FOS)	Structure	Stratum (Disposition)
C-2303S (1)	65.3	11.3	0.26	No Structure (Northeast of CB)	Stratum Sand 1 (no structure)
C-2323S (1)	54.2	11.5	0.58	No Structure (Southeast of CB)	Stratum Sand 1 (no structure)

Source: SSAR Table 2.5.4-81

Figure 1 - Boring/CPT locations with loose sand layer and the corresponding distances with respect to the eastern embankment



RAI 02.05.05-8:**Question:**

SSAR Subsection 2.5.5.2.5.4 describes the seismic stability and post-earthquake deformations of the slopes. Based on design criteria, the post-earthquake residual strength is equal to 0.8 times the static value. In accordance with 10 CFR 100.23(d)(4), please explain how this criterion is satisfied for the VCS site.

Response:

Two different sets of soil parameters were used in the analyses of the seismic stability and the seismic deformations of the cooling basin embankments.

Regarding the seismic stability of the cooling basin embankments, SSAR Subsection 2.5.5.2.2.6 describes the adopted methodology. Based on this methodology, the residual undrained shear strengths of the fill materials, foundation clays, and foundation sands were taken as 80 percent of the pre-earthquake strengths shown on SSAR Figures 2.5.5-10 (Line B), 2.5.5-12 (Line C), and 2.5.5-13 (Line A), respectively. For foundation sands, $c' = 0.32$ ksf, being 80 percent of the recommended $c' = 0.4$ ksf (refer to SSAR Subsection 2.5.5.1.9.1.3). As presented in SSAR Table 2.5.5-2, the following soil parameters were used in the seismic stability analyses. Thus, based on the adopted design criterion, the post-earthquake residual strengths are equal to 0.8 times the static values and this criterion is satisfied for the VCS site.

Post-Earthquake Case	
Stratum	Geotechnical properties
Embankment Fill	$\tau/\sigma = 0.62$, $s_{u\min} = 1030$ psf, $\phi' = 0^\circ$, $\gamma = 134$ pcf
Foundation Clays	$\tau/\sigma = 0.36$, $s_{u\min} = 530$ psf, $\phi' = 0^\circ$, $\gamma = 126$ pcf
Foundation Sands	$s_u = 320$ psf, $\phi' = 33^\circ$, $\gamma = 126$ pcf

Regarding the evaluation of the seismic deformations of the embankments, SSAR Subsection 2.5.5.2.5.4 describes the adopted methodology. The same critical slip surfaces obtained during the steady state condition using Slope/W were analyzed with various horizontal accelerations and zero vertical acceleration to compute the yield accelerations that result in a factor of safety against shear failure equal to 1.0. As presented in SSAR Table 2.5.5-2, the following effective soils parameters were used in the seismic deformation analyses. Thus, based on the adopted design criterion, strength parameters equal to the static values are used and this criterion is satisfied for the VCS site.

Steady-State Seepage Case ^(a)	
Stratum	Geotechnical Properties
Embankment Fill	$s_u=0$ psf, $\phi'=30^\circ$, $\gamma=134$ pcf
Foundation Clays	$s_u=0$ psf, $\phi'=28^\circ$, $\gamma=126$ pcf
Foundation Sands	$s_u=400$ psf, $\phi'=40^\circ$, $\gamma=126$ pcf

- (a) The case of "slope deformation during the design seismic event" uses the same strength parameters as the "steady-state seepage case," to solve for the yield acceleration of each profile.

Associated ESPA Revisions:

In response to this RAI, SSAR Subsection 2.5.5.2.5.4 will be revised in a future revision to the ESPA as follows:

2.5.5.2.5.4 Seismic Stability and Post-Earthquake Deformations

The Makdisi/Seed approach ([Reference 2.5.5-5](#)) is selected from the table in [Reference 2.5.5-1](#) for the evaluation of earthquake-induced slope deformations of embankment dams. In this approach, the expected seismic deformations of the slopes are calculated as a function of:

- The pseudo-static yield coefficient of horizontal acceleration that brings the factor of safety against sliding of the slope down to 1.0
- The average effective acceleration within the soil mass
- The ratio of the yield acceleration to the average effective embankment acceleration
- The duration of strong ground shaking

Preliminary design criteria call for an earthquake characterized by peak ground acceleration equal to 0.10g at the base of the embankment associated with a moment magnitude = 7.6 earthquake.

Critical slip surfaces and yield accelerations are computed using the same soil parameters selected for the steady state seepage analysis in Table 2.5.5-2. The results are shown in Figures 2.5.5-29 through 2.5.5-33 and are summarized in Table 2.5.5-8.

The average effective ground acceleration within the embankment is a function of the amplitude of the ground acceleration at the crest of the embankment. The maximum value of the crest acceleration is a function of several variables, namely: embankment height, fill stiffness, and characteristics of the earthquake ground motion. Experience shows that the ratio of crest acceleration to ground surface acceleration at the base of the embankment may range between less than one to approximately two. A conservative value of the ratio equal to two is adopted for the slope deformation evaluations. Figure 9 in [Reference 2.5.5-5](#) shows that the average effective embankment acceleration is equal to approximately 45 percent of the crest acceleration.

Consequently, the average effective embankment acceleration in this case is equal to ground acceleration at the base of the embankment (0.10g) x crest amplification factor (2) x reduction factor between crest and average effective embankment acceleration (0.45) = 0.09g.

Table 2.5.5-9 lists the values of the yield acceleration/average effective acceleration ratios for the five embankment sections. Figure 14 in the Makdisi/Seed reference (Reference 2.5.5-5) shows that the expected seismic displacements for the listed ratios are negligible.

Post-earthquake slope stabilities are analyzed using the methodology described in SSAR Subsection 2.5.5.2.2.6. The results are presented on Figures 2.5.5-34 through 2.5.5-38 and are summarized in Table 2.5.5-10 (outboard slope). In all cases the calculated factors of safety exceed 1.5.

ATTACHMENT 6

SUMMARY OF REGULATORY COMMITMENTS

(Exelon Letter to USNRC, NP-11-0036, dated August 4, 2011)

The following table identifies commitments made in this document. (Any other actions discussed in the submittal represent intended or planned actions. They are described to the NRC for the NRC's information and are not regulatory commitments.)

COMMITMENT	COMMITTED DATE	COMMITMENT TYPE	
		ONE-TIME ACTION (Yes/No)	Programmatic (Yes/No)
Exelon will revise the VCS ESPA SSAR Section 2.5.4 to incorporate the change shown in the enclosed response to the following NRC RAI: 02.05.04-13 (Attachment 1)	Revision 1 of the ESPA SSAR and ER planned for no later than March 31, 2012	Yes	No
Exelon will revise the VCS ESPA SSAR Section 2.5.4 to incorporate the change shown in the enclosed response to the following NRC RAI: 02.05.04-14 (Attachment 2)	Revision 1 of the ESPA SSAR and ER planned for no later than March 31, 2012	Yes	No
Exelon will revise the VCS ESPA SSAR Section 2.5.5 to incorporate the change shown in the enclosed response to the following NRC RAI: 02.05.05-8 (Attachment 5)	Revision 1 of the ESPA SSAR and ER planned for no later than March 31, 2012	Yes	No